

A Spatially and Temporally Correlated Fading Channel Model for Smart Antenna Applications

Seon-Taek Kim*, Nam-Il Yun*, Han-Wook Jung**,
Han-Kyu Park* *Regular Members*

※ This paper was financially supported by Korea Telecom.

ABSTRACT

In this paper a new fading model is proposed, which is well consistent with the real environment of smart antenna applications since it is spatially and temporally correlated simultaneously. The new model(STCFM: Spatially and Temporally Correlated Fading Model) is derived statistically in spatio-temporal domain so that it can provide high accuracy in the evaluation of the smart antenna system. As will be seen, the simulation results agree well with the theory.

I. Introduction

The increasing demand for the mobile communication services with high spectral efficiency has motivated development of new techniques. SDMA(Spatial Division Multiple Access) using a smart antenna has been proposed as a potential answer to this challenge. Recently benefits of smart antennas have been demonstrated by many authors[1]-[3]. For a primary work of such complex systems the simulation provides a cost-effective solution. Channel models including the spatial parameters have been proposed in recent papers. Roughly the spatial models fall into two groups. One is sum of scattered waves[4][5], and the other is measurement-based model[6][7]. These models,

however, have a common drawback of imperfection in the statistical property on which the reliability of a simulation result depends heavily. It is, therefore, urgently needed to develop a model which satisfies both the statistical and spatial properties of the real fading channel simultaneously. In this paper a new model is proposed, which has statistical strictness in both time and space domains.

II. Spatio-Temporal Channel Model

A. Spatial correlation between array elements

Figure 1 shows a wireless communication system employing an array antenna. All signals from the mobile arrive at the base station within AOS(Angle Of Spread) of $\pm \Delta$ at DOA(Direction Of Arrival) of ϕ . We assume that the array is linear with M omni-directional elements of identical spacing, d . Assuming flat fading and the narrow-bandwidth plane waves at

*Radio Communications Research Center, Yonsei Univ.

**Wireless Communication Research Lab., Korea Telecom

論文番號:97119-0329

接受日字:1997年 3月 29日

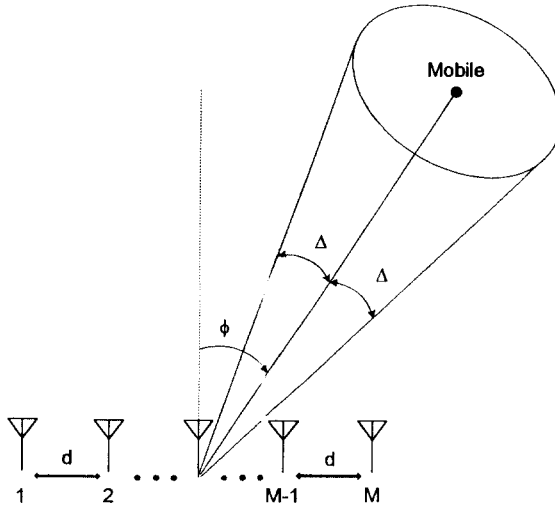


Fig. 1. Mobile channel for array antenna applications with directional informations, DOA and AOS.

the array input, the output signals at the array element m due to the transmission $s(t)$ from the DOA of ϕ are given by

$$r_m(t) = a_m s(t) \quad 1 \leq m \leq M \quad (1)$$

where

$$a_m = \sum_n g_n e^{j\theta_n} e^{j2\pi(m-1)\frac{d}{\lambda} \sin \phi_n} = x_m + jy_m \quad (2)$$

where g_n 's and θ_n 's are the random scattering amplitudes and phases respectively, ϕ_n is the angle of arrival of the n th ray, and λ is the wavelength of the carrier frequency. Then, the $M \times 1$ array response becomes

$$A = [a_1 \ a_2 \ \dots \ a_M]^T \quad (3)$$

where the superscript denotes transpose. Now, we seek the correlation between the following random variables,

$$\begin{aligned} a_i &= x_i + jy_i, & i &= 1, \dots, M \\ a_k &= x_k + jy_k, & k &= 1, \dots, M \end{aligned} \quad (4)$$

Assuming the probability density function of ϕ_n as, for all n

$$p(\phi_n) = \begin{cases} \frac{1}{2\Delta} & -\Delta + \phi \leq \phi_n \leq \Delta + \phi \\ 0 & \text{elsewhere} \end{cases} \quad (5)$$

, we obtain the following formulas for the spatial correlations[8]

$$\frac{1}{\sigma^2} E[x_i x_k] = \tilde{R}_{xx}(i-k) = \frac{1}{\sigma^2} E[y_i y_k] = \tilde{R}_{yy}(i-k) \quad (6)$$

$$= J_0(z(i-k)) + 2 \sum_{n=1}^{\infty} J_{2n}(z(i-k)) \cos(2n\phi) \frac{\sin(2n\Delta)}{2n\Delta}$$

$$\frac{1}{\sigma^2} E[y_i x_k] = \tilde{R}_{yx}(i-k) = -\frac{1}{\sigma^2} E[x_i y_k] = -\tilde{R}_{xy}(i-k) \quad (7)$$

$$= 2 \sum_{n=0}^{\infty} J_{2n+1}(z(i-k)) \sin((2n+1)\phi) \frac{\sin((2n+1)\Delta)}{(2n+1)\Delta}$$

where $z = 2\pi d/\lambda$, and $\sigma^2 = \frac{1}{2} \sum_n E[g_n^2]$. Then, the spatial correlation coefficient ρ becomes

$$\rho = \sqrt{\tilde{R}_{xx}^2 + \tilde{R}_{xy}^2} \quad (8)$$

Defining a $2M \times 1$ augmented vector of A as $A_a = [x_1 \ y_1 \ x_2 \ y_2 \ \dots \ x_M \ y_M]^T$, the $2M \times 2M$ spatial correlation matrix $R_s = E[A_a A_a^T]$ can be obtained as in [8]

$$\frac{R_s}{\sigma^2} = \begin{bmatrix} I_{2 \times 2} & D_1 & D_2 & \dots & D_{M-1} \\ D_1^T & I_{2 \times 2} & D_1 & \dots & D_{M-2} \\ D_2^T & D_1^T & I_{2 \times 2} & \dots & D_{M-3} \\ \vdots & \vdots & \vdots & \dots & \vdots \\ D_{M-1}^T & D_{M-2}^T & D_{M-3}^T & \dots & I_{2 \times 2} \end{bmatrix} \quad (9)$$

where the 2×2 matrix

$$D_{|i-k|} = \begin{bmatrix} \tilde{R}_{xx}(i-k) & -\tilde{R}_{xy}(|i-k|) \\ \tilde{R}_{xy}(|i-k|) & \tilde{R}_{xx}(i-k) \end{bmatrix} \quad i, k=1, \dots, M \quad (10)$$

B. Temporally correlated fading process

We assume the power spectral density of the Jake's model[9]

$$S_c(f) = \begin{cases} \frac{2\sigma^2}{\pi f_D \sqrt{1-(f/f_D)^2}} & |f| < f_D \\ 0 & |f| > f_D \end{cases} \quad (11)$$

where f_D is the maximum Doppler spread. Here, (11) is implemented using a FIR(Finite Impulse Response) filter as following: Let $h(m)$, $0 \leq m \leq N_t - 1$, be the impulse response of the FIR shaping filter we seek, and let $H(n)$, $0 \leq n \leq N_t - 1$ be the corresponding DFT(Discrete Fourier Transform) coefficients. Obviously, $S_c(f)$ in (11) can be expressed in the form of DFT as

$$H_d(n) = \begin{cases} \frac{\sigma}{\sqrt{\frac{\pi}{2} f_D \sqrt{1-(n f_s / N_t f_D)^2}}} & 0 \leq n < N_t = \frac{N_t f_D}{f_s} \\ 0 & N_t \leq n \leq N_h = \frac{N_t - 1}{2} \end{cases} \quad (12)$$

for odd N_t with $N_t \geq f_s / (f_s - 2f_D)$, and the sampling rate $f_s > 2f_D$ where $N_t f_D / f_s$ has been assumed as an integer. Since the real and imaginary parts of (2) must be independent each other, $h(m)$ should be real. If we set

$$\begin{aligned} H(n) &= H_d(n) & 0 \leq n \leq N_h \\ H(n) &= H(N_t - n) & N_h < n < N_t \end{aligned} \quad (13)$$

then, the resulting filter will have real coefficients. From the definition of the inverse DFT $h(m)$ becomes

$$h(m) = \frac{1}{N_t} \left\{ H(0) + 2 \sum_{n=1}^{N_h} \text{Re} [H(n) e^{-j2\pi \frac{mn}{N_t}}] \right\} \quad (14)$$

Each tap coefficient $\tilde{h}(m)$ after the Kaiser windowing is divided $\sqrt{\sum_{m=0}^{N_t-1} \tilde{h}^2(m)}$ to obtain the normalized coefficient $\bar{h}(m)$.

III. The implementation of spatially and temporally correlated fading process

Let q_1, q_2, \dots, q_{2M} be the $2M \times 1$ eigenvectors corresponding to the distinct eigenvalues $\lambda_1, \lambda_2, \dots, \lambda_{2M}$ of the spatial correlation matrix R_s / σ^2 , respectively. Let a $2M \times 1$ column vector U be $[u_1 \ u_2 \ \dots \ u_{2M}]^T$ where each element u_m is a zero-mean Gaussian random variable with variance of 1/2. Then, a random process V with the desired spatial correlation R_s can be obtained by

$$\begin{aligned} V &= [v_1 \ v_2 \ \dots \ v_{2M}]^T \\ &= \frac{R_s^{1/2}}{\sigma^2} U \end{aligned} \quad (15)$$

where

$$\frac{R_s^{1/2}}{\sigma^2} = Q \Lambda^{1/2} Q^A \quad (16)$$

where $Q = [q_1, q_2, \dots, q_{2M}]$ and Λ is the diagonal matrix of $\text{diag}(\sqrt{\lambda_1}, \sqrt{\lambda_2}, \dots, \sqrt{\lambda_{2M}})$. Finally, the $M \times 1$ spatially and temporally correlated complex channel vector A of (3) is given by

$$A(n) = \sum_{m=0}^{N_t-1} \bar{h}(m) W(n-m) \quad (17)$$

where the $M \times 1$ complex $W(n)$'s are statistically independent each other with the m th element given by $w_m(n) = v_{2m-1}(n) + jv_{2m}(n)$. Hereafter we call this channel model as STCFM(Spatially and Temporally Correlated Fading Model).

IV. Numerical Results

A. Spatial properties of STCFM

To validate the STCFM the DOA performance is evaluated first. The testbed is a 2-element array antenna with element spacing $d = 0.5\lambda$. As well known, when a non-faded LOS(Line Of Sight) signal arrives, the

array antenna has the only maximum output at the DOA of the signal in the range of $|\phi| \leq 90^\circ$ with the corresponding unique beam pattern. If we set the AOS narrow enough, the fading signals in the two branches are highly correlated and the spatial signature resembles that of a LOS signal. Using this principle we can measure the DOA performance of STCFM without using a complex direction-finding algorithm. $\Delta = 5^\circ$ is enough for this purpose. For three different DOA's ($\phi = -60^\circ, 0^\circ,$ and 45°) the results are illustrated in Fig. 2. The solid lines are for the non-faded LOS. Each dotted line for the fading signal has been obtained by averaging the 1×10^5 spatial signatures from (17). It agrees well with the beam pattern of the corresponding LOS, having the same maximum peak. It assures that the DOA of STCFM is well defined. The two patterns deviate in the null. To form a null the phase difference between the signals in the two branches must be 180° with the same magnitudes as in the LOS case. Since the fading signals, although highly correlated, are random process, they cannot be out of phase exactly so that the

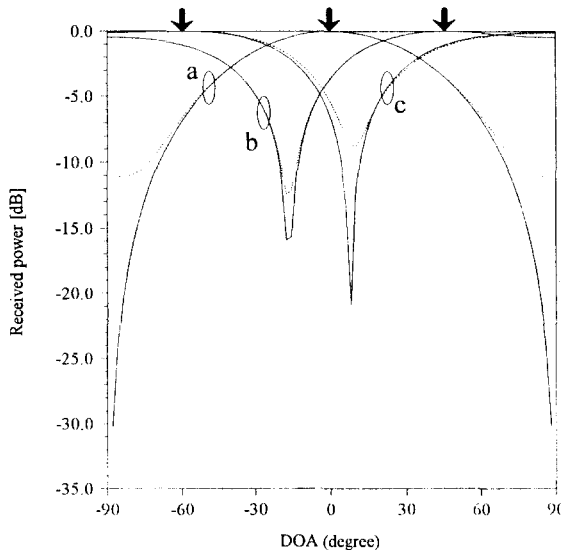


Fig. 2. DOA property of STCFM
 (—— : LOS, : fading, DOA $\phi =$ a: 0° , b: 45° ,
 c: -60°)

deep null does not occur.

Secondly, the AOS property has been observed. To the authors' knowledge, it seems that a convenient method for the measurement of the AOS in a fading environment has not been developed so far. Thus, we have to rely on a straight-forward solution which scans the received signals with a very narrow-beam array antenna. The linear array we consider, however, has a wide beamwidth because it consists of the omni-directional elements. The beamwidth can be narrowed by either increasing the number of the array elements, or widening the element-spacing. Increasing d , however, generates the grating lobes. If we consider $\Delta \leq 30^\circ$, $d = \lambda$ does not introduce the grating lobes in the scanning area. Also, we have increased the element number to 48. The resulting 3-dB beamwidth is about 1° , and the powers at $\pm 1^\circ$ from the maximum peak are 14.6 dB below, from which we have determined the scanning resolution as 2° . For three different AOS's ($2\Delta = 12, 20,$ and 40°) the narrow beam has been scanned in the range $|\phi| \leq 30^\circ$ with DOA $= 0^\circ$ and equal power in all cases. The results have been obtained by averaging over 1×10^5 snap-shots and are given in Fig. 3. It can be seen that the measured 3-dB beamwidth is exactly equal to the corresponding AOS. The power angular density is lowered by 3 dB as Δ doubles, which is well consistent with the physical consideration because we have assumed equal power for all three case. For DOA $= 0^\circ$ and AOS $\geq 10^\circ$ we consider, the spatial correlation coefficient ρ becomes less than 0.4 with $d \geq 4\lambda$, in which case the faded signals in the two branches can be seen as statistically independent. Since the length of the array is 47λ , the spatial signature in our case is very different from in the LOS condition. So, the patterns in Fig. 3 have some errors from a rectangular form assumed in (5). The reason for the relatively high-level sidelobes outside the AOS can be explained in the same vein. The errors, therefore, are due to the scanning method itself. Taking this into account, it is concluded that the AOS characteristic of STCFM is also well defined as the DOA.

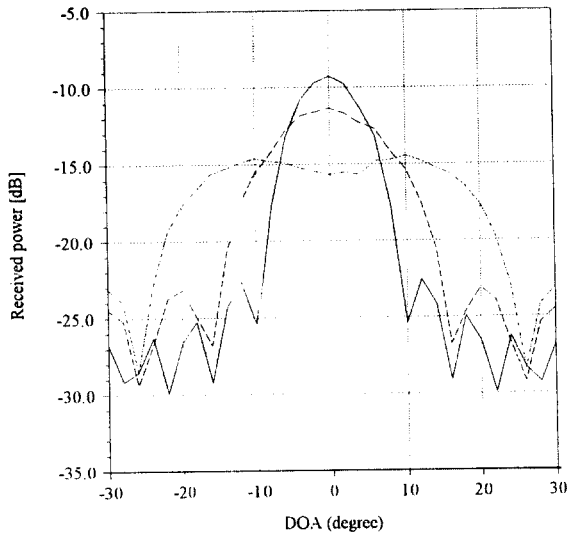


Fig. 3. AOS property of STCFM
(AOS $2\Delta =$ — : 12° , - - - : 20° , - · - · : 40°)

B. Statistical properties of STCFM

The previous two tests were to validate the spatial property while this subsection is for the temporal statistical characteristics of STCFM. To this end we have evaluated temporal ACF(Auto-Correlation Function). The testbed is a 2-element array with $d = 0.5\lambda$. The DOA and the AOS are 0° and 20° , respectively. The simulation has been performed on the first of the two array elements and is plotted in Fig. 4. The simulating

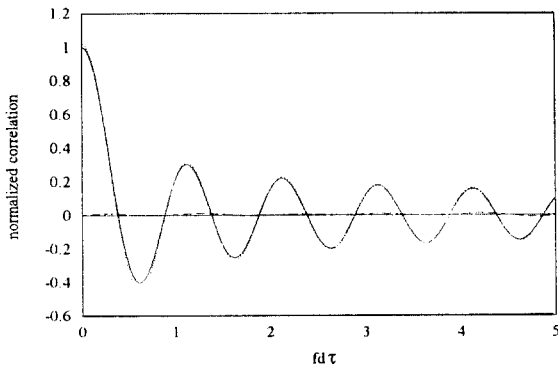


Fig. 4. ACF as a function of time delay τ
($R_{xx}(\tau)$ — : theory, - - - : simulation, $R_{xy}(\tau)$ — : theory, - - - : simulation).

runs are 4×10^6 . The ACF of STCFM agrees well with the theory.

C. Application to maximal ratio diversity system

The probability distributions of the output SNR, as the model is applied to the two-branch MRC(maximal ratio combining), are given in Fig. 5 to demonstrate the spatial correlation property. The DOA and d are 0° and 0.382λ , respectively. The averaging has been performed over 4×10^6 runs. The theory and the simulations are in tight agreement. The four different spatial correlation coefficients $\rho = 1, 0.89, 0.77,$ and 0.0024 have been obtained by adjusting Δ to $0, 20, 30,$ and 180° , respectively.

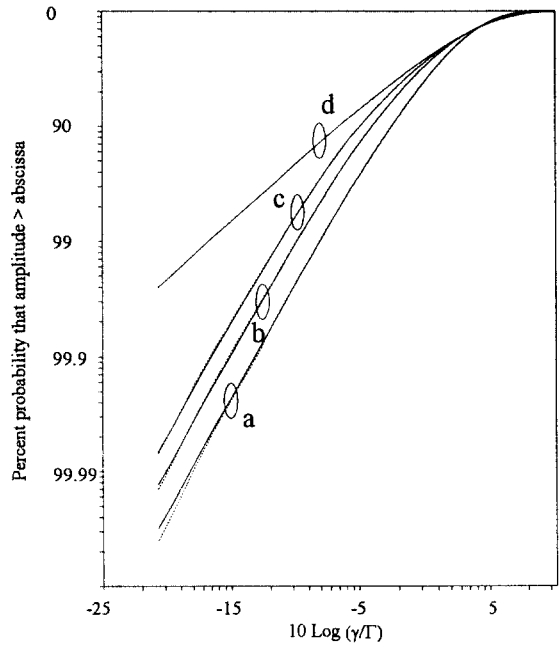


Fig. 5. Probability distributions of output SNR γ for two-branch MRC with branch SNR T
(— : theory, - - - : simulation, $\rho =$ a: 0.0024 , b: 0.77 , c: 0.89 , d: 1).

V. Conclusion

In this paper we have extended the present tem-

poral fading channel model to the space domain. The development of smart antenna system for the mobile communication services has required a new channel model which is spatially and temporally correlated simultaneously. The conventional channel models have been focused mainly on the realization of the directional informations of DOA or AOS. Hence the statistical properties such as the spatial correlation between the array branches or the temporal autocorrelation are incomplete in these models. To overcome these drawbacks the newly proposed STCFM has been derived from the statistical point of view incorporating all the necessary informations in space and time domain. As demonstrated in the simulations the STCFM shows strictness in both the physical consistency and the statistical property.

참 고 문 헌

1. G. V. Tsoulos, M. A. Beach, and S. C. Swales, "Application of Adaptive Antenna Technology to Third Generation Mixed Cell Radio Architectures", in *IEEE Veh. Technol. Conference Proc.*, Stockholm, June 8-10, pp. 615-619, 1994.
2. J. C. Liberti, Jr., and T. S. Rappaport, "Analytical Results for Capacity Improvements in CDMA", *IEEE Trans. Veh. Technol.*, vol. 43, no. 3, pp. 680-690, Aug. 1994.
3. A. F. Naguib, A. Paulraj, and T. Kailath, "Capacity Improvement with Base-Station Antenna Arrays in Cellular CDMA", *IEEE Trans. Veh. Technol.*, vol. 43, no. 3, pp. 691-698, Aug. 1994.
4. S. P. Stapleton, X. Carbo, and T. Mckeen, "Spatial Channel Simulator for Phased Array", in *IEEE Veh. Technol. Conference Proc.*, Stockholm, June 8-10, pp. 1789-1792, 1994.
5. J. Fuhl, and A. F. Molisch, "Capacity Enhancement and BER in a Combined SDMA/TDMA System", in *IEEE Veh. Technol. Conference Proc.*, Atlanta, GA, USA, Apr. 28-May 1, pp. 1481-1485, 1996.
6. S. P. Stapleton, X. Carbo, and T. Mckeen, "Tracking and Diversity for a Mobile Communications Base Station Array Antenna", *IEEE Veh. Technol. Conference Proc.*, Atlanta, GA, USA, Apr. 28-May 1, pp. 1695-1699, 1996.
7. H. Liu, and G. Xu, "Closed-Form Blind Symbol Estimation in Digital Communications", *IEEE Trans. Signal Processing*, vol. 43, no. 11, pp. 2714-2723, Nov. 1995.
8. J. Salz, and J. H. Winters, "Effect of Fading Correlation on Adaptive Arrays in Digital Wireless Communications", in *IEEE Int. Conference on Comm. Proc.*, Geneva, Switzerland, May 23-26, pp. 1768-1774, 1993.
9. W. C. Jakes, *Microwave Mobile Communications*, New York, John Wiley & Sons, 1974.



김 선 택(Seon-Taek Kim) 정회원
 1970년 2월 10일생
 1992년 2월: 연세대학교 전자공학과 졸업(공학사)
 1994년 2월: 연세대학교 본대학원 전자공학과 졸업(공학석사)
 1994년 3월~현재: 연세대학교 본대학원 전자공학과 박사과정 재학
 ※주관심분야: 마이크로파 응용, 적응배열안테나, 위성 및 이동통신



윤 남 일(Nam-Il Yun) 정회원
 1961년 4월 10일생
 1985년 2월: 연세대학교 전자공학과 졸업(공학사)
 1987년 2월: 연세대학교 본대학원 전자공학과 졸업(공학석사)
 1995년 9월~현재: 연세대학교 본대학원 전자공학과 박사과정 재학
 1987년 2월~1994년 2월: 삼성전자 통신연구소 근무(선임연구원)
 1994년 3월~현재: 명지전문대학 전자과 조교수
 ※주관심분야: 마이크로파 소자해석, 이동통신



정 한 옥(Han-Wook Jung) 정회원

1961년 1월 22일생

1982년 2월: 경북대학교 전자공
학과 졸업(공학사)

1984년 2월: 경북대학교 대학원
전자공학과 졸업(공
학석사)

1991년 8월~1996년 9월: Dept.
of Electrical and Computer Eng., State University of
New York at Buffalo(Ph.D.)

1985년 12월~현재: 한국통신 연구개발본부 무선통신
연구소 팀장

※주관심분야: 무선통신, 가입자접속망, 광통신

박 한 규(Han-Kyu Park)

정회원

1996년 12월호 동 논문지 페이지 3214 참조